The "Wimple": Rippled Deformation of a Fluid Drop Caused by Hydrodynamic and Surface Forces during Thin Film Drainage

Lucy Y. Clasohm,[†,‡] Jason N. Connor,[†,||] Olga I. Vinogradova,[‡,§] and Roger G. Horn*[,†]

Ian Wark Research Institute, University of South Australia, Mawson Lakes, Adelaide, SA 5095, Australia, Max Planck Institute for Polymer Research, Ackermannweg 10, 55128 Mainz, Germany, and A. N. Frumkin Institute of Physical Chemistry and Electrochemistry, 31 Leninsky Prospect, 119991, Moscow, Russia

Received April 1, 2005. In Final Form: June 16, 2005

It is well-known that hydrodynamic pressures in a thin draining liquid film can cause inversion of the curvature of a drop or bubble surface as it approaches another surface, creating a so-called "dimple". Here it is shown that a more complicated rippled shape, dubbed a "wimple", can be formed if a fluid drop that is already close to a solid wall is abruptly pushed further toward it. The wimple includes a central region in which the film remains thin, surrounded by a ring of greater film thickness that is bounded at the outer edge by a barrier rim where the film is thin. This shape later evolves into a conventional dimple bounded by the barrier rim, which then drains in the normal way. During the evolution from wimple to dimple, some of the fluid in the thicker part of the film ring flows toward the central region before eventually draining in the opposite direction. Although the drop is pressed toward the wall, the central part of the drop moves away from the wall before approaching it again. This is observed even when the inward push is too small to create a wimple.

1. Introduction

It is well-known that forces acting between two colloidal particles immersed in an aqueous medium play important roles in determining the behavior of colloidal systems. Forces include equilibrium surface forces and hydrodynamic forces. The equilibrium forces are reasonably well understood from DLVO theory[1] and information gleaned from direct measurements.[2] Extensive efforts have also gone into investigating hydrodynamic forces, both theoretically[3−6] and experimentally.[7−13] The majority of previous work on colloidal forces has assumed that interacting particles or surfaces are nondeformable, although some attention has been paid to elastically deformable surfaces.[14−19]

The assumption that interacting bodies are either rigid or only deform elastically becomes unrealistic in colloidal systems where fluid drops are involved, such as emulsions, foams, and flotation separation processes. In such cases another factor, drop (or bubble) deformation, comes into play. Deformation is strongly coupled to the surface and hydrodynamic forces, so it becomes a very important consideration in interactions involving drops and/or bubbles. The body of theoretical and experimental work investigating colloidal forces between deformable fluid objects is much less than that for rigid objects, although there is a growing literature in this area.[20−30]

* Corresponding author. E-mail: roger.horn@unisa.edu.au.
† University of South Australia.
‡ Max Planck Institute for Polymer Research.
§ A. N. Frumkin Institute of Physical Chemistry and Electrochemistry.
|| Present address: PELM Centre, Central Queensland University, Gladstone, Queensland 4680, Australia.

(1) Hunter, R. J. *Foundations of Colloid Science*; 2nd ed.; Oxford University Press: Oxford, 2001.
(2) Israelachvili, J. N. *Intermolecular and Surface Forces*; 2nd ed.; Academic Press: London, 1992.
(3) Russel, W. B.; Saville, D. A.; Schowalter, W. R. *Colloidal Dispersions*; Cambridge University Press: Cambridge, UK, 1989.
(4) Cox, R. G. *Int. J. Multiphase Flow* **1974**, *1*, 343−371.
(5) Davis, R. H.; Schonberg, J. A.; Rallison, J. M. *Phys. Fluids* **1989**, *1*, 77−81.
(6) Vinogradova, O. I. *Langmuir* **1995**, *11*, 2213.
(7) Chan, D. Y. C.; Horn, R. G. *J. Chem. Phys.* **1985**, *83*, 5311−5324.
(8) Israelachvili, J. N. *J. Colloid Interface Sci.* **1986**, *110*, 263−271.
(9) Tonck, A.; Georges, J.-M.; Loubet, J.-L. *J. Colloid Interface Sci.* **1988**, *126*, 150−163.
(10) Craig, V. S. J.; Neto, C.; Williams, D. R. M. *Phys. Rev. Lett.* **2001**, *87*, 054504.
(11) Bonaccurso, E.; Kappl, M.; Butt, H.-J. *Phys. Rev. Lett.* **2002**, *88*, 076103.
(12) Horn, R.; Vinogradova, O. I.; Mackay, M. E.; Phan-Thien, N. *J. Chem. Phys.* **2000**, *112*, 6424−6433.
(13) Vinogradova, O. I.; Yakubov, G. E. *Langmuir* **2003**, *19*, 1227−1234.
(14) Hughes, B. D.; White, L. R. *J. Chem. Soc., Faraday Trans. 1* **1980**, *76*, 963−978.
(15) Seraysol, J.-M.; Davis, R. H. *J. Colloid Interface Sci.* **1986**, *114*, 54−66.
(16) Attard, P.; Parker, J. L. *Phys. Rev. A* **1992**, *46*, 7959−7971.
(17) Vinogradova, O. I.; Feuillebois, F. *J. Colloid Interface Sci.* **2000**, *221*, 1−12.
(18) Vinogradova, O. I.; Feuillebois, F. *Langmuir* **2002**, *18*, 5126−5132.
(19) Vinogradova, O. I.; Feuillebois, F. *J. Colloid Interface Sci.* **2003**, *268*, 464−475.
(20) Butt, H.-J. *J. Colloid Interface Sci.* **1994**, *166*, 109−117.
(21) Ducker, W. A.; Xu, Z.; Israelachvili, J. *Langmuir* **1994**, *10*, 3279−3289.
(22) Miklavcic, S. J.; Horn, R. G.; Bachmann, D. J. *J. Phys. Chem.* **1995**, *99*, 16357−16364.
(23) Fielden, M. L.; Hayes, R. A.; Ralston, J. *Langmuir* **1996**, *12*, 3721−3727.
(24) Horn, R. G.; Bachmann, D. J.; Connor, J. N.; Miklavcic, S. J. *J. Phys.: Condens. Matter* **1996**, *8*, 9483−9490.
(25) Aston, D. E.; Berg, J. C. *J. Colloid Interface Sci.* **2001**, *235*, 162−169.
(26) Bhatt, D.; Newman, J.; Radke, C. J. *Langmuir* **2000**, *17*, 116−130.
(27) Yang, S.-M.; Leal, L. G.; Kim, Y.-S. *J. Colloid Interface Sci.* **2002**, *250*, 457−465.
(28) Dagastine, R. R.; Stevens, G. W.; Chan, D. Y. C.; Grieser, F. *J. Colloid Interface Sci.* **2004**, *273*, 339.

10.1021/la0508588 CCC: $30.25
Published on Web 07/29/2005

In efforts to better understand the connection between colloidal forces (including hydrodynamics) and deformation of a fluid surface, the behavior of a fluid drop approaching another fluid drop or a solid wall in a liquid has been studied over several decades and by several groups. In many of these studies a phenomenon called "dimpling" has been observed[31−39] and analyzed theoretically.[27,35,40−47] This occurs when hydrodynamic pressure builds up in the thin film of liquid as it flows (or "drains") from the gap between the drop and the other surface. When the approach speed is sufficiently high and the separation is small, this pressure can be large enough to invert the curvature of the drop, forming a dimple. The dimple is bounded by a so-called barrier rim, which is the circle of minimum separation between the two surfaces. The rate at which liquid can flow through the thin gap at the barrier rim restricts the drainage of the intervening liquid film. This can become the rate-limiting process in determining the approach and possible aggregation or coalescence of drops, or their attachment to surfaces.

Previous investigations of dimpling have investigated the deformation created when a drop (or bubble) approaches another surface from a large initial separation. We are unaware of any previous work that has addressed the question of dimple development starting from other initial conditions. In this paper, we explore what happens when a drop is initially at rest close to a solid surface, separated by a nanometer-scale wetting film of background fluid, and then the drop and solid are driven toward each other. Our results show that a dimple can form, but in the early stages the drop surface has a more complex rippled form that we call a *wimple* (an obscure but real word, one of whose meanings is a ripple on the surface of a liquid).

The wimple has never been predicted theoretically, nor has it been observed in previous experiments. It may have important consequences for understanding wetting and dewetting; two-phase flow in microfluidic systems; elastohydrodynamic effects; and coalescence of deformable objects including drops, bubbles, and perhaps biological cells. In particular, our results show that the central part of a fluid drop actually moves away from the solid before it moves back toward it, even though the center of mass of the drop moves toward the wall rather than away from it. For this to occur, the immersion fluid flows initially inward toward the central part of the wetting film that separates the solid from the drop, and then flows outward again.

2. Experimental Method

The experiments were carried out using the same technique as previous investigations of dimpling carried out by two of us.[39] We used a modified surface force apparatus (SFA) in which a flat horizontal mica surface is mounted above a mercury drop held at the end of a vertical capillary, 3 mm in diameter. The mica and the mercury are both immersed in aqueous electrolyte solution. The mica can be moved with nanometer control using a differential spring arrangement and two micrometers driven by microstepping motors (Nanomover, Melles Griot, USA), while the capillary remains stationary. The separation between mica and mercury surfaces (i.e., the aqueous film thickness) is measured by optical interference fringes of equal chromatic order (FECO).[48] This method allows detailed measurements of the drop shape, i.e., the film thickness as a function of radial (horizontal) distance from the axis of symmetry, which is a vertical line through the center of the capillary and perpendicular to the mica surface. Reflection FECO are recorded on a Sony UVW-1400P Betacam SP PAL video recorder (Sony Corporation, Japan) and later transferred to a computer using a frame grabber (Fidelity 200 DT3852 Frame Processor, Data Translation Inc., USA). Subsequent image analysis of each frame gives a resolution of about 0.5 nm in film thickness, 1 μm in radial position, and 40 ms in time.[49]

A similar arrangement, but with an air bubble in place of the mercury drop,[49,50] was also used for some experiments. Reflection FECO are still observable in this configuration, albeit giving less resolution in film thickness.[51] Only qualitative observations have been made with the air bubble at this stage, but these provided important corroboration of the mercury drop results to be presented below.

A three-electrode system was used to apply a potential to the mercury drop to control the surface forces, which are dominated by electrical-double-layer forces at the film thicknesses (50−250 nm) investigated in these experiments. A hollow cylinder of platinum gauze (25 × 25 mm, 52 mesh 99.9% Pt, Aldrich, USA) was placed around the mercury drop as a counter electrode, and a saturated calomel reference electrode (SCE) was connected to the apparatus using a Luggin capillary. An Autolab potentiostat (PGSTAT-30, Eco Chemie BV, Metrohm, The Netherlands) was used to control the potential applied to the mercury working electrode. During the experiment, a negative potential (either −910 or −440 mV vs SCE) was applied to give the mercury a negative surface charge and hence create a repulsive force between the drop and the solid[52] (mica is known to be negatively charged in water).

Before the start of each experimental run, the mica surface was moved toward the mercury until the mercury drop flattened slightly due to the repulsive force.[22] In this configuration an equilibrium thin film of electrolyte was formed between the mercury and mica (Figure 1). After allowing time to equilibrate at this position, the mica was driven further toward the mercury drop. The movement was applied for a preset displacement at a comparatively rapid speed (100 μm/s). Displacements investigated in different experimental runs were 1, 5, 10, and 20 μm; hence the duration of each displacement step was at most 0.2 s. The deformation of the drop as a function of time was recorded and analyzed following each displacement step.

Mica was freshly cleaved to a thickness of ∼5 μm and partially silvered on its upper surface to satisfy the optical requirements

(29) Gunning, A. P.; Mackie, A. R.; Wilde, P. J.; Morris, V. J. *Langmuir* **2004**, *20*, 116−122.
(30) Carnie, S. L.; Chan, D. Y. C.; Lewis, C.; Manica, R.; Dagastine, R. R. *Langmuir* **2005**, *21*, 2912−2922.
(31) Derjaguin, B. V.; Kussakov, M. M. *Acta Physicochim. URSS* **1939**, *10*, 25−30.
(32) Platikanov, D. *J. Phys. Chem.* **1964**, *68*, 3619−3624.
(33) Hartland, S. *Chem. Eng. Sci.* **1969**, *65*, 82−89.
(34) Burrill, K. A.; Woods, D. R. *J. Colloid Interface Sci.* **1973**, *42*, 15−34.
(35) Joye, J.-L.; Miller, C. A.; Hirasaki, G. J. *Langmuir* **1992**, *8*, 3083−3092.
(36) Hewitt, D.; Fornasiero, D.; Ralston, J.; Fisher, L. R. *J. Chem. Soc., Faraday Trans.* **1993**, *89*, 817−822.
(37) Tsekov, R.; Ruckenstein, E. *Colloids Surf., A* **1994**, *82*, 255−261.
(38) Goodall, D. G.; Gee, M. L.; Stevens, G. *Langmuir* **2002**, *18*.
(39) Connor, J. N.; Horn, R. G. *Faraday Discuss.* **2003**, *123*, 193−206.
(40) Frankel, S. P.; Mysels, K. J. *J. Phys. Chem.* **1962**, *66*, 190−191.
(41) Hartland, S.; Robinson, J. D. *J. Colloid Interface Sci.* **1977**, *60*, 72−81.
(42) Dimitrov, D. S.; Ivanov, I. B. *J. Colloid Interface Sci.* **1978**, *64*, 97−106.
(43) Lin, C.-Y.; Slattery, J. C. *AIChE J.* **1982**, *28*, 147−156.
(44) Chen, J.-D. *J. Colloid Interface Sci.* **1984**, *98*, 329−341.
(45) Yiantsios, S. G.; Davis, R. H. *J. Fluid Mech.* **1990**, *217*, 547−573.
(46) Abid, S.; Chesters, A. K. *Int. J. Multiphase Flow* **1994**, *20*, 613−629.
(47) Klaseboer, E.; Chevaillier, J. P.; Gourdon, C.; Masbernat, O. *J. Colloid Interface Sci.* **2000**, *229*, 274−285.
(48) Tolansky, S. *Surface Microtopography*; Longmans, Green & Co. Ltd.: London, 1960; pp 42−53.
(49) Connor, J. N. Measurement of Interactions between Solid and Fluid Surfaces. Ph.D. Thesis, University of South Australia, Adelaide, 2001.
(50) Pushkarova, R. A.; Horn, R. G. *Colloids Surf., A: Physicochem. Eng. Aspects* **2005**, *261*, 147−152.
(51) Connor, J. N.; Horn, R. G. *Rev. Sci. Instrum.* **2003**, *74*, 4601−4606.
(52) Connor, J. N.; Horn, R. G. *Langmuir* **2001**, *17*, 7194−7197.

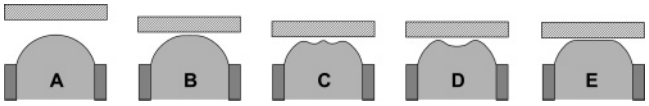

Figure 1. Schematic figure of the experiment showing a mercury drop (or air bubble) held by a fixed capillary below a horizontal solid surface (mica) which can be moved vertically down toward the drop. Initially the solid is moved from A to B, and then it is given time to equilibrate at B, where the drop is slightly flattened by repulsive double-layer interaction with the solid. The solid is then moved rapidly to position C and held there. The response of the drop is to form a rippled "wimple" (C) that evolves into a normal dimple (D) and then eventually flattens out again (E). Previous drainage experiments have driven one or other surfaces continuously from a large separation (A) to position D without pausing at position B or observing the wimple (C).

of the FECO method before being glued onto a flat silica disk. Water used to make up electrolyte (1 mM KCl) was polished by reverse osmosis, ion exchange, and activated charcoal cartridges before being distilled using a subboiling still manufactured from fused quartz (Quartz & Silice PB15, France). AnalaR grade KCl (99.5%, BDH Merck) was purchased and used as received. Electronic grade mercury (99.9999%, Sigma-Aldrich) was purchased from Aldrich and purified before use by placing it under nitric acid and bubbling high-purity oxygen through it for 24 h before rinsing the acid away with copious amounts of distilled water.[49]

3. Results

The initial configuration is stationary with the mercury drop close to, but not contacting, the mica surface. The drop is flattened slightly by a repulsive double-layer force, and the initial aqueous film thickness in the central region is close to that at which the positive disjoining pressure due to the double-layer repulsion is equal to the Laplace pressure in the drop (~280 Pa).[22] For some experiments a potential of −910 mV was applied to the mercury, giving a large negative charge and a situation that we term "strong repulsion". At this applied potential the surface potential on mercury is negative with a magnitude of at least 250 mV,[52] interacting with mica whose surface potential in 1 mM KCl is around −80 to −100 mV.[53] The strong double-layer repulsion gave an initial minimum film thickness of 51 nm. In other experiments a potential of −440 mV created a "weak repulsion", and the initial minimum film thickness was 45 nm.

The separation between mercury and mica is plotted against the radial distance from the symmetry axis as a function of time. Time $t = 0$ s is set at the last video frame before the mica displacement step is made. We choose to plot the surface separation in the $-y$ direction on the graphs, because this reflects the actual orientation of the mercury drop surface (see Figure 1).

A. Strong Repulsion. *(i) 20 μm Step.* Response of the mercury drop to a 20 μm step in the presence of strong repulsion is shown in Figure 2. Before the step, the initial drop is somewhat flattened over a radius of about 10 μm. After the displacement is made, the curvature of the drop near $r = 0$ did not invert immediately to form a dimple, unlike the case when the mica is driven toward the mercury from far away.[39] Instead, the central portion remains close to the mica and maintains a convex curvature in the early stages. At the same time, the outer regions of the drop approach the mica, forming shoulders that will eventually develop into a barrier rim. Between the central region and the shoulders, a thicker ring of fluid is trapped by the sudden approach of the drop and

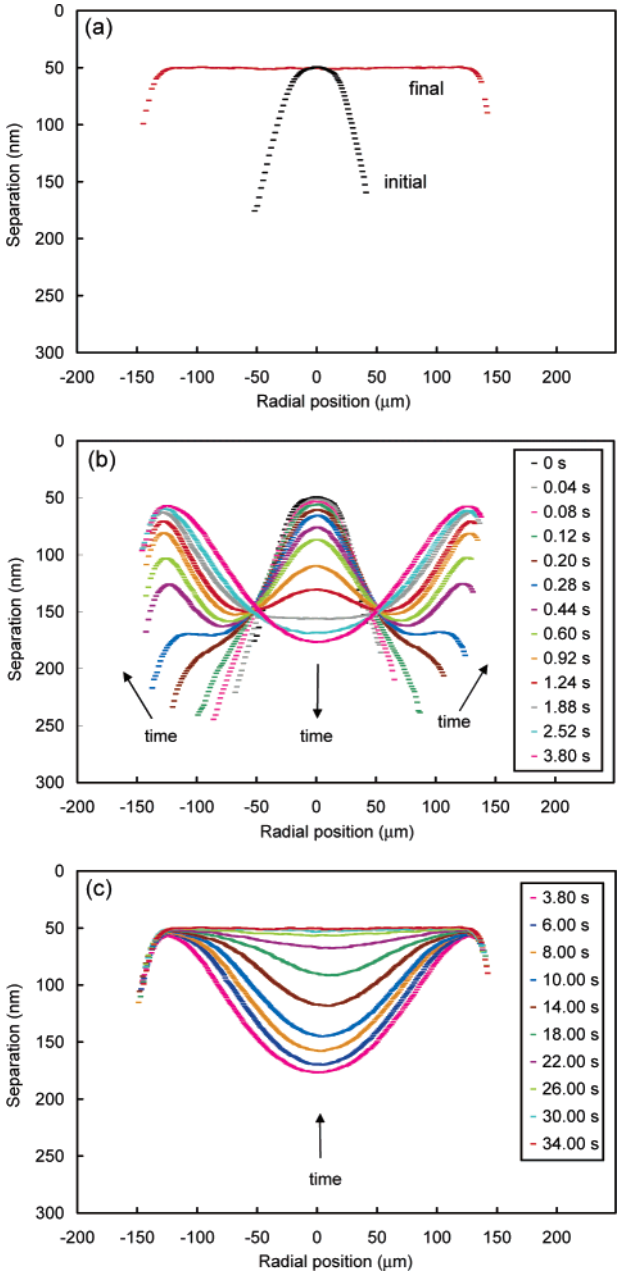

Figure 2. (a) Initial and final profiles of a mercury drop before (black) and long after (red) a flat mica surface is moved down toward it in a single rapid step. Each symbol (−) represents an experimental data point. Note the 1000-fold difference between vertical and horizontal scales, which exaggerates the apparent curvature of the drop surface. These two profiles correspond to the configurations sketched in Figure 1B and 1E, respectively. (b) Formation of a wimple at −910 mV (vs SCE) applied potential, giving a strong repulsion. Step size: 20 μm. Measurement times are 0, 0.04, 0.08, 0.12, 0.20, 0.28, 0.44, 0.60, 0.92, 1.24, 1.88, 2.52, and 3.80 s. (c) Later evolution of the wimple under the same conditions. Measurement times are 3.80 (the same curve repeated from part b), 6, 8, 10, 14, 18, 22, 26, 30, and 34 s.

wall. This results in an annular region of concave curvature separating the shoulders from the central region, both of which remain convex. Only after the formation of a distinct barrier rim does the central region gradually pull away from the solid surface and invert its curvature to concave, until after about 2−3 s a normal dimple has formed. During this phase some of the aqueous film trapped in the thicker ring must be flowing toward the central axis. At intermediate times (between about 0.4 and 1 s in this case) the

(53) Pashley, R. M. *J. Colloid Interface Sci.* **1981**, *83*, 531−546.

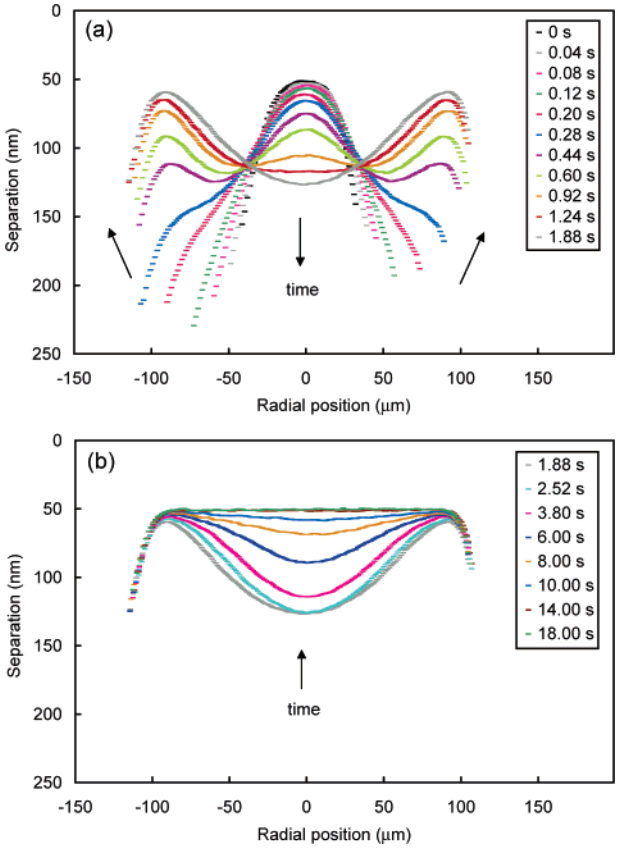

Figure 3. (a) Formation of a wimple at −910 mV (vs SCE) applied potential, giving a strong repulsion. Step size: 10 μm. Measurement times are 0, 0.04, 0.08, 0.12, 0.20, 0.28, 0.44, 0.60, 0.92, 1.24, and 1.88 s. (b) Later evolution of the wimple under the same conditions. Measurement times are 1.88 (repeated), 2.52, 3.80, 6, 8, 10, 14, and 18 s.

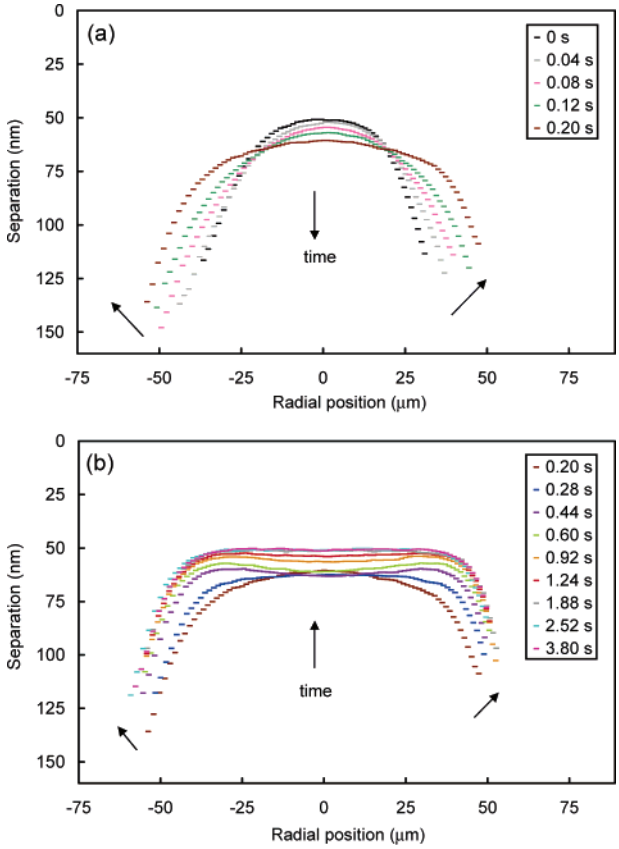

Figure 4. Evolution of drop shape following a 5 μm step with applied potential of −910 mV (vs SCE). (a) Measurement times of 0, 0.04, 0.08, 0.12, and 0.20 s. (b) Measurement times of 0.20 (repeated), 0.28, 0.44, 0.60, 0.92, 1.24, 1.88, 2.52, and 3.80 s.

drop surface has a complex rippled shape with a "W" profile (which helped suggest the name "wimple" to describe this phenomenon).

After the wimple has evolved into a normal dimple with concave curvature, the dimple amplitude decreases with time, water flows out past the barrier rim, and in a little more than 30 s the drop reaches its final equilibrium shape. The drop is flattened at the same film thickness as initially (because this is set by the balance of disjoining pressure and Laplace pressure, neither of which was changed in making the step[54]), but now with a much larger flattened radius of about 125 μm.

(ii) 10 μm Step. Drop deformation in response to a smaller step (10 μm) is shown in Figure 3. The behavior of the mercury drop is similar to the case of the 20 μm step size, but with a smaller degree of deformation. The formation of the wimple takes about 0.4 s, but it evolves into a dimple more quickly than the previous case, in less than 2 s. When the dimple forms, the maximum film thickness at the center of the drop is only 125 nm compared to 180 nm for the larger step. The evolution of the dimple takes about half the time needed previously—about 18 s. A flattened radius of 90 μm is obtained once the equilibrium is reached at the same equilibrium film thickness (51 nm) as before the drop deformation. This result suggests that the degree of wimple formation is determined by how much the surfaces are pushed together. A more pronounced wimple and a larger dimple is formed for a greater displacement of the drop relative to the surface. A bigger displacement also results in a longer drainage time of the dimple, and a larger flattened area at the final equilibrium position.

(iii) 5 μm Step. The drop's response to a rapid 5 μm displacement of the mica surface is shown in Figure 4. No obvious wimple is observed, although a weak dimple forms after about 0.4 s (Figure 4b). Before the dimple has formed, the central, slightly flattened region of the drop moves away from the solid surface, despite the fact that the mica has been driven toward it. The weak dimple drains comparatively quickly, and after ~4 s the drop reaches final equilibrium with a film thickness of 51 nm again and a flattened radius of about 70 μm.

(iv) 1 μm Step. The behavior following a 1 μm step is qualitatively the same as with the 5 μm step, but with a smaller degree of deformation. Again, no wimple is formed with a small step, but the central part of the aqueous film increases in thickness after the step before decreasing again to its original value. This indicates that water flows toward the central axis initially, and then away again. The variation of the film thickness is only a few nanometers, whereas it was about 10 nm in the previous case. The final flattened radius is the smallest of all the step sizes, at about 30 μm. The time that it takes to reach equilibrium is similar to the previous case, about 3.8 s.

Taken together, the observations suggest that there is a critical step size that will cause the formation of a wimple, and under these conditions it is between 5 and 10 μm.

B. Weak Repulsion. Similar experiments were conducted with a potential of −440 mV (vs SCE) applied to

(54) In fact, the drop volume remains constant during the step, and the Laplace pressure does change slightly. However, the deformation is very small, on the millimeter scale of the whole drop. A numerical calculation of the drop shape shows that the change in its Laplace pressure would be 2% at most. For a double-layer repulsion with a Debye length of 10 nm, this would correspond to a shift in the equilibrium separation of 0.2 nm.

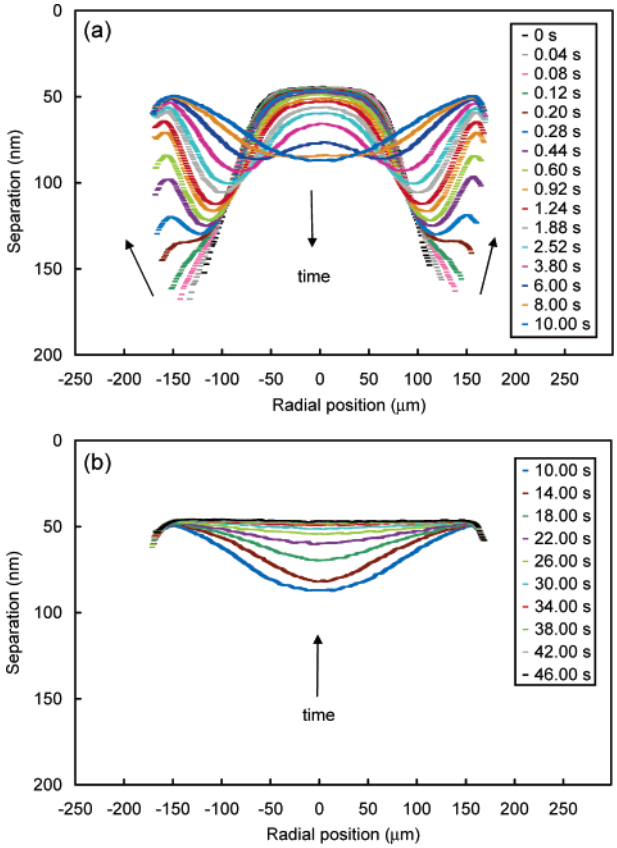

Figure 5. (a) Formation of a wimple at −440 mV (vs SCE) applied potential, giving a weak repulsion. Step size: 20 μm. Measurement times are 0, 0.04, 0.08, 0.12, 0.20, 0.28, 0.44, 0.60, 0.92, 1.24, 1.88, 2.52, 3.80, 6, 8, and 10 s. (b) Later evolution of the wimple under the same conditions. Measurement times are 10 (repeated), 14, 18, 22, 26, 30, 34, 38, 42, and 46 s.

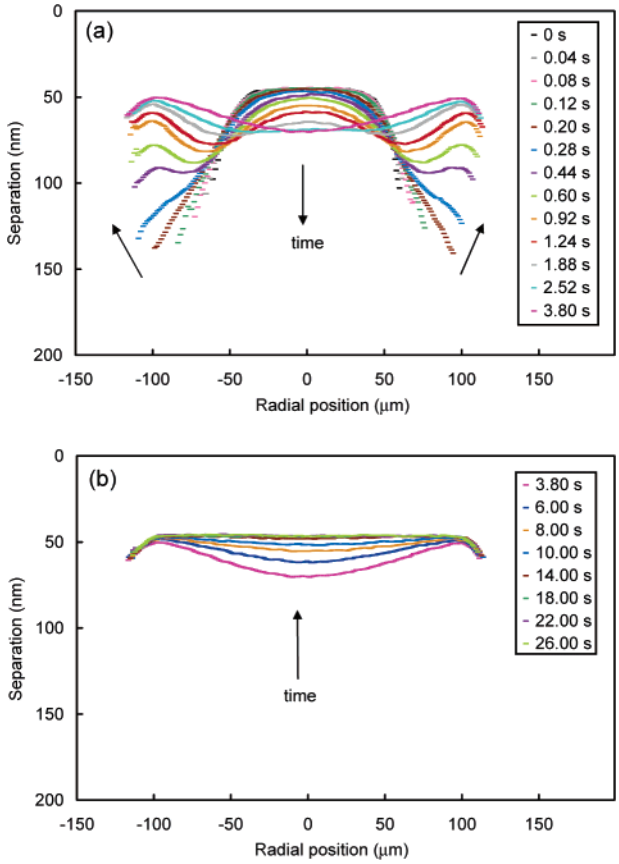

Figure 6. (a) Formation of a wimple at −440 mV (vs SCE) applied potential, giving a weak repulsion. Step size: 10 μm. Measurement times are 0, 0.04, 0.08, 0.12, 0.20, 0.28, 0.44, 0.60, 0.92, 1.24, 1.88, 2.52, and 3.80 s. (b) Later evolution of the wimple under the same conditions. Measurement times are 3.80 (repeated), 6, 8, 10, 14, 18, 22, and 26 s.

the mercury drop, which gives the mercury a surface potential of about −35 mV[52] and creates a weaker repulsion between the mica and mercury surfaces. The results are presented in Figures 5 and 6 for steps of 20 and 10 μm, respectively. Wimple formation is observed in both cases.

In both Figures 5 and 6 the initial configuration had a larger flat area, with radii of 45 and 35 μm, respectively. In addition, as an inevitable consequence of the weaker repulsion, there was a reduced equilibrium film thickness between the mica and the mercury drop before and long after the step was made. Both of these factors contribute to the transition from a wimple to a dimple taking a longer time, now ~10 s rather than 2−3 s for the strong repulsion experiments at the same step sizes (Figures 2 and 3). The time taken for the central part of the drop to pull away from the mica surface is restricted by hydrodynamic drag on this part of the drop. Such drag would be increased by having a thinner film, and also by having a larger initial flattened area.

With weak repulsion the film drainage after a dimple has formed is also slower. This effect has been noted before,[32,35,36,39,44] and is also explained by the fact that, with reduced repulsion, the gap between the barrier rim and the mica is smaller, causing greater restriction on the flow rate of the water.

Consistent with the earlier results, comparison of Figures 5 and 6 shows that a larger step size results in a more distinct wimple, a larger amplitude dimple, a longer time required to drain water from the dimple, and a greater flattened area in the final configuration. Similarly to the strong repulsion case, no wimple was observed for smaller displacement steps.

4. Discussion

Our results show that dimpling and thin film drainage can be more complicated than the usual picture which assumes that the process starts with deformable drops approaching surfaces from a large distance. If the presence of a repulsive force between the fluid drop and a nearby surface allows the drop to be initially stationary close to it, an abrupt force or displacement that presses the drop closer results in the formation of a wimple that later evolves into a dimple. Wimple refers to a shape whose profile has convex curvature (as seen from the side of the film) at the center surrounded by a region of concave curvature and eventual convex curvature again outside the deformed region of the drop. A dimple has a simpler profile with only concave curvature at the center.

Perhaps the most interesting and important aspect of this phenomenon is that the central part of the intervening liquid film grows thicker before thinning again to its initial value. This can only occur if some of the liquid in the film first flows toward the central axis, before later draining out in the opposite direction.[33]

The flow direction is associated with hydrodynamic pressures in the film, which in turn can be related to the curvature of the drop's surface that bounds the film. From the Young−Laplace equation it is known that the pressure difference between the aqueous film and the interior of the mercury drop is proportional to the interfacial curvature. Convex curvature corresponds to lower pressure in the film than in the drop. Hence, when a wimple is present, the film pressure near $r = 0$ and near the

shoulder (or barrier rim) is low, while it is high in the intermediate annular region where curvature is concave. The film pressure has two components: hydrodynamic pressure and disjoining pressure arising from electrical-double-layer forces between the bounding surfaces of mica and mercury. The disjoining pressure is a decreasing function of film thickness, which means that this component is maximal in the same regions of the film where the convex curvature is greatest and the total film pressure is least: the center and in the neighborhood of the barrier rim. Hence the hydrodynamic pressure must be minimal in those parts of the film. Conversely, in the intermediate region between the center and the barrier rim where curvature is concave and the film thickness is greater, there is high total film pressure and low disjoining pressure. This means that the hydrodynamic pressure (strictly, the difference in hydrodynamic pressures between the aqueous film and the mercury immediately on the other side of the interface) must be high in this region. Hence fluid in the film flows from this region toward regions of lower hydrodynamic pressure, which are found both at the center ($r = 0$) and near (as well as outside) the barrier rim. That is, some of the fluid from the thick annular region of the film flows toward the thin central part, while some flows outward toward (and past) the barrier rim. Only after the inward flow has created a thick bell in the film's central region—the normal dimple shape with concave curvature at the center—does the fluid flow outward only, allowing the dimple to drain.

This behavior is highlighted in Figure 7. Part a plots the evolution of the film thickness at the central axis and at the barrier rim for 10 and 20 μm steps, clearly showing that the former grows by as much as 200% before decaying back to its initial value. The barrier rim only forms some time (~0.5 s) after the step is made, and then it approaches the final film thickness more rapidly than the central film thickness does, as observed for a conventional dimple.

Figure 7b shows that the central part of the film has qualitatively the same behavior, i.e., thickening followed by thinning, even for small step sizes for which no wimple is observed. It seems remarkable that when the drop is pushed abruptly toward the wall, the response of fluid in the film is first to flow inward toward the central region and thicken that part of the film, before later reversing its flow and draining out again. The above discussion about regions of concave and convex curvature no longer holds. Nevertheless, a quantitative calculation of interfacial curvature and hydrodynamic pressure distribution[55] shows that this pressure has a local minimum at $r = 0$ and a maximum at some finite value of r, driving flow toward both small r and large r simultaneously shortly after the step is made (before flowing only outward in the later stages as the new equilibrium configuration is approached).

These results have been obtained in a particular experimental configuration which differs from previous studies in that the initial configuration of a drop is at rest and is already close to another surface. The previous studies, in which the drop approaches a surface from a large distance, are designed to model a collision between a drop and another surface. The present arrangement is more relevant for a drop (or bubble) close to a surface receiving a sudden impulse. For example, if a bubble sitting below a horizontal hydrophilic surface were to have a second bubble collide with it from below, the result would be something like what we have presented here. (This would occur whether or not the bubbles coalesce: in that case a similar impulsive force would result from suddenly increasing the buoyancy force pressing the coalesced bubble against the surface.)

(55) Clasohm, L. Y. Ph.D. Thesis, University of South Australia, 2005.

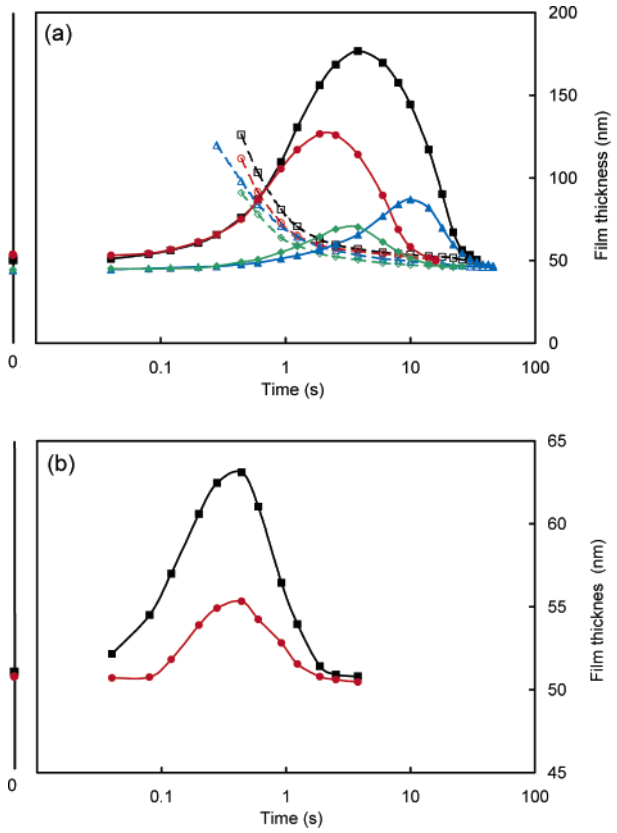

Figure 7. (a) Film thickness at the center of symmetry (filled symbols) and at the barrier rim (empty symbols), plotted as a function of time. (A logarithmic scale is used simply to compress the long-time data.) Black squares: strong repulsion, 20 μm step. Red circles: strong repulsion, 10 μm step. Blue triangles: weak repulsion, 20 μm step. Green diamonds: weak repulsion, 10 μm step. (b) Film thickness at the center of symmetry for smaller steps in the strong repulsion case. Black squares: 5 μm step. Red circles: 1 μm step. Note the expanded vertical scale of (b).

A reversal of radial flow direction during thin film drainage involving deformable fluid drops has been noted before by Hartland,[33] but in general it is not a possibility that has been discussed in theoretical investigations of the dimpling phenomenon. Our results show that flow reversal can certainly occur, and depending on the initial configuration, it could be an important aspect of the problem. Indeed, given that the central film thickness is observed to increase before returning to its equilibrium value even with small displacement steps that cause no wimple and only a faint dimple, such flow reversal appears to be the norm rather than the exception in these experiments.

Mercury has unusual properties, and it is conceivable that one or more of these could be a cause of the unusual deformation we have reported here:

(a) It has an unusually high interfacial tension against the background fluid, water (about 420 mJ/m^2). The interfacial tension opposes drop deformation, and perhaps a high value somehow favors a type of deformation that has not been observed in other experiments on drops approaching surfaces.

(b) The unusually high density of mercury would cause greater inertial effects in the drop's flow than would the density of other fluids, so it is reasonable to ask whether

fluid inertia has something to do with the wimpling phenomenon.

(c) Mercury's viscosity (1.55 mPa·s) is comparable to that of water, which means that fluid flow within the drop is coupled to flow in the aqueous film. Hartland[33] speculated that the phenomenon of film thickening at the central axis during evolution of a normal dimple results from inward flow of the film caused by coupling to circulatory flow within the drop.

To understand whether any of these factors is significant, comparable experiments were carried out with an air bubble in place of the mercury drop. Although detailed data were not obtained, qualitative observations showed that a wimple does form in this case, too. This proves that the inward-then-outward fluid flow in the film is not a consequence of fluid inertia in the drop/bubble or of coupled flow of the film to internal circulation within the drop (bubble); nor is it caused by high interfacial tension. The fact that wimpling is observed with two fluids as different as mercury and air suggests that this is a general phenomenon, applicable (for example) to the bubble/surface interactions as suggested above.

5. Conclusion

We have presented data showing the deformation of a mercury drop due to the sudden approach of a mica sheet from an initial position that is already close to the mercury, in the presence of a repulsive surface force. A new phenomenon has been observed, called wimpling, in which the drop surface forms a central island of convex curvature surrounded by a moat of concave curvature, before evolving into a normal dimple of concave curvature. It appears that the sudden approach causes a dimple to form, similar to what is commonly observed when a drop approaches a surface at sufficiently high speed from a large initial separation. However, when the initial separation is small, a wimple appears to form en route to forming the dimple, because the central part of the drop is slow to pull away from its position close to the opposing surface. The central part of the film therefore thickens, slowly at first, before later thinning again to its original thickness. This means that in the early part of the process some of the liquid in the film flows *toward* the central axis ($r = 0$) before reversing its flow direction and flowing outward to larger r. The rate of initial film thickening near the center is limited by hydrodynamic resistance in that part of the film, which is initially the thinnest part. The hydrodynamic resistance is higher and the thickening rate lower when the initial film thickness is low and/or its quasi-flat area is large.

There is a critical step size below which the wimple does not form. However, the phenomenon of initial film thickening at the center, followed by thinning, occurs even for small steps. Somewhat counterintuitively, the response of the drop to an impulsive force pushing it toward a neighboring surface is first to increase its minimum separation from the surface and only later to return to its equilibrium separation. Fluid in the background liquid flows into the central part of the film initially before later draining out again. Overall, our results demonstrate that dimpling and thin film drainage involving deformable drops can be more complicated than what is allowed for in the conventional descriptions of the problem.

Acknowledgment. This work has been supported by the Australian Research Council Special Research Centre for Particle and Material Interfaces, the Deutsche Forschungsgemeinschaft through its "Micro and Nanofluidics" program (Vi 243/1-1), and the International Max Planck Research School for Polymer Materials Science through the award of a visiting scholarship to L.Y.C. We are grateful to Terry Blake, Steve Carnie, Derek Chan, Miao Chen, François Feuillebois, and Rogerio Manica for helpful discussions.

LA0508588